PARAMETRIC OPTIMIZATION OF THE ELECTRICAL DISCHARGE DRILLING OPERATION OF TITANIUM ALLOY FOR HOLE DILATION AND DRILLING SPEED

TỐI ƯU HÓA THÔNG SỐ CÔNG NGHỆ CỦA QUÁ TRÌNH KHOAN XUNG HỢP KIM TITANIUM XEM XÉT ĐẾN ĐỘ MỞ RỘNG CỦA LỖ VÀ TỐC ĐỘ GIA CÔNG

Vu Ngoc Nha[1], Le Van An[2], Luong Thi Lan Huong[3], Nguyen Trung Thanh[1,*]

DOI: http://doi.org/10.57001/huih5804.2025.125

ABSTRACT

The electrical discharge drilling (EDD) process is an effective solution to produce small holes in difficult-to-cut materials. In this work, the EDD parameters, including the current (I), the gap voltage adjustor (G), the pulse on time (Ton), and the pulse off time (Tof) are optimized to reduce the hole dilation (HD) and increase the drilling speed (V). The EDD trials were conducted for the titanium grade 4 using the Box-Behnken method. The Gaussian process regression (GPR) approach is used to develop the correlations of the EDD responses. Lastly, the best values for the EDD parameters were found using the non-dominated sorting genetic algorithm II (NSGA-II). The results showed that the optimal I, G, Ton, and Tof are 13A, 8, 65µs, and 55µs, respectively. The HD was reduced by 32.6%, while the V was enhanced by 76.7% at the optimal point, as compared to the initial values. The outcomes could be applied to the practical EDD process of titanium grade 4 for improving the drilled quality and productivity. The proposed approach could be used to solve optimization problems for other EDD processes.

Keywords: *EDD, hole dilation, drilling speed, Gaussian process regression, titanium grade 4.*

TÓM TẮT

Quá trình khoan xung là một giải pháp hiệu quả để tạo ra các lỗ nhỏ trên các vật liệu có tính gia công thấp. Trong nghiên cứu này, các thông số của quá trình khoan xung, bao gồm cường độ dòng điện, hệ số điều chỉnh điện áp, thời gian bật xung và thời gian tắt xung được tối ưu hóa để giảm độ mở rộng của lỗ và tăng tốc độ gia công. Các thí nghiệm khoan xung được tiến hành đối với vật liệu titannium tinh khiết cấp 4 thông qua phương pháp Box-Behnken. Phương pháp hồi quy Gaussian (GPR) được sử dụng để mô tả các hàm mục tiêu. Giá trị tối ưu của các thông số công nghệ được xác định với sự trợ giúp của thuật toán di truyền đa mục tiêu (NSGA-II). Kết quả chỉ ra rằng giá trị tối ưu của cường độ dòng điện, hệ số điều chỉnh điện áp, thời gian bật xung và thời gian tắt xung lần lượt là 13A, 8, 65µs và 55µs. Độ mở rộng của lỗ có thể giảm khoảng 32,6%, trong khi tốc độ gia công được cải thiện 76,7%, so với giá trị ban đầu. Kết quả nghiên cứu có thể được áp dụng vào qúa trình khoan xung thực tế của vật liệu titan tinh khiết cấp 4 để cải thiện chất lượng và năng suất gia công. Phương pháp tối ưu đề xuất có thể được sử dụng để giải quyết các bài toán tối ưu cho các quá trình khoan xung khác.

Từ khóa: *Khoan xung, độ mở rộng của lỗ, tốc độ gia công, phương pháp hồi quy Gaussian, vật liệu titanium.*

[1]Faculty of Mechanical Engineering, Le Quy Don Technical University, Vietnam
[2]Faculty of Engineering and Technology, Nguyen Tat Thanh University, Vietnam
[3]Faculty of Foreign Languages, Le Quy Don Technical University, Vietnam
[*]Email: trungthanhk21@mta.edu.vn
Received: 20/01/2025
Revised: 15/4/2025
Accepted: 28/5/2025

1. INTRODUCTION

The electrical discharge drilling (EDD) is widely applied to produce holes with small diameters and different geometries on hard-to-cut materials. The plasma channel between the anode and cathode with high temperature (8,000 to 12,000°C) is produced during the drilling time. The thermal energy is used to melt and vaporize the material, while the debris is flushed away by dielectric fluid. The EDD can be used to machine any conductive materials irrespective of their mechanical properties such as strength and hardness. Therefore, the EDD can be used to produce holes in hard-to-cut materials such as polycrystalline diamond, nickels, and titanium alloys.

Many former researchers have performed the parameter-based optimizations for enhancing the technical responses of the EDD processes. The ANFIS models of the material removal rate, electrode wear rate, taper angle, hole circularity, and hole dilation (HD) of the drilled Inconel-825 alloy were developed in terms of the current (I), pulse on-time (Ton), pulse off-time (Tof), and electrode diameter [1]. The authors stated that the responses could be precisely predicted using the developed correlations. The impacts Ton, I, Tof, voltage, and tool electrode speed on the material removal rate, average surface roughness, and power consumption of the drilled Waspaloy were explored [2]. The results indicated that the I, Ton, and Tof were the most influential factors, contributing 50.45%, 34.29%, and 33.09% to the responses. The ANFIS models of the specific drilling energy, HD, and the tapper ratio were proposed in terms of the I, Ton, Tof, gap voltage adjustor (G), voltage, capacitance parallel connection, and servo sensitivity selection [3]. The outcomes presented that the specific drilling energy, HD, and tapper ratio were reduced by 10.13%, 34.46%, and 11.63%, respectively, as compared to initial values. The impacts of the EDD parameters on the HD and machining speed of the drilled Inconel-718 alloy were explored using the response surface methodology [4]. The experimental results showed that the responses were primarily affected by the voltage and I, respectively. The mathematical models for the material removal rate and surface roughness for the vibration-assisted electrical discharge drilling of Titanium alloy were developed in terms of the I, Ton, Tof, tool rotation speed, and vibration amplitude [5]. The prediction errors of less than 9% indicated that the developed models were accurate. The Taguchi method was used to reduce the overcut and circularity of drilled Mg alloy holes [6]. The author stated that the optimal I, Ton, and Tof were 3A, 50µs, and 52µs, respectively, while the optimal overcut and circularity were 93.48µm and 0.992, respectively.

The ANN was used to present the correlations of the material removal rate and surface roughness for the drilled Inconel 718 alloy [7]. The experimental results indicated that the I and Ton had an effect on the performance of the drilling process considerably. The impacts of the I, Ton, voltage, dielectric fluid pressure, and tool rotation speed on the drilling speed, linear tool wear, the side gap thickness, and the aspect ratio of holes were explored [8]. The results indicated that higher values of the I and Ton could be used to ensure the hole accuracy. The optimal values of the GAP, capacitance parallel connection, and servo sensitivity selection were selected to obtain the improvements in the HD, material removal rate, and drilled energy [9]. The findings revealed the optimal values of the GAP, capacitance parallel connection, and servo sensitivity selection were 6, 5, and 4, respectively. The impacts of the voltage, feed rate, and electrode rotation speed on the material removal rate, overcut, and taper angle for the drilled Inconel 718 alloy were investigated [10]. The analysis showed that voltage was the most significant factor influencing all the responses. A new EDD process having the diamond electrode was developed to minimize the roughness and circularity of the drilled nickel alloy [11]. The significant enhancements of the technical responses were achieved, as compared to the traditional ones. Singh et al. stated that the EDD operation employing the rotary electrode provided a higher material removal rate and a lower tool wear rate, as compared to the traditional one [12]. Yadav et al. emphasized that the oxygen gas assisted-EDD process has an efficient contribution to enhance the production rate, roughness, and hole characteristics [13]. The ANN models of the material removal rate, tool wear rate, overcut, and tapper angle were proposed for the drilled polymer [14]. The authors presented that the optimal I, Ton, Tof, and fluid pressure were 4A, 25µs, 25µs, and 0.6MPa, respectively.

However, the EDD process has still some inherent problems exist, such as low efficiency and geometric errors. As a result, the predictive models of the HD and drilling speed (V) of the EDD process of the titanium alloy have not been developed. Moreover, the optimal values of the I, G, Ton, and Tof have not been selected to reduce the HD and increase the V.

The optimization approach is then presented. After that, the experimental setup and results are discussed. Lastly, some findings are described.

2. OPTIMIZATION APPROACH

2.1. EDD parameters and responses

To ensure the quality and machining efficiency, the hole dilation and drilling speed are considered as important EDD responses. The HD is computed as:

$$HD = D_D - D_e \quad (1)$$

where D_e is the original diameter of the electrode. D_D is the average diameter of drilled hole and calculated as:

$$D_D = \frac{D_1 + D_2 + ... + D_n}{n} \quad (2)$$

where D_i and n are the drilled diameters at the entry at the i_{th} location and the number of measuring points, respectively.

The V is computed as:

$$V = \frac{H}{t} = \frac{H_1 + H_2 + ... + H_n}{n} \quad (3)$$

where the H and t are the drilled length and drilling time, respectively. H_i presents the drilled length at the i_{th} position.

Table 1. EDD parameters and their levels

Symbol	Parameters	level-1	level 0	level +1
I	Current (A)	12	25	38
G	Gap voltage adjustor	2	5	8
Ton	Pulse on time (µs)	55	70	85
Tof	Pulse off time (µs)	55	70	85

The factors considered are the current, gap voltage adjustor, pulse on time, and pulse off time. The EDD parameters and their levels are presented in Table 1. The ranges of these factors are selected based on the characteristics of the EDD machine. The optimizing issue can be described as follows:

Find X = [I, G, Ton, Tof]

Maximizing V; Minimizing HD

Constraints: 12 ≤ I ≤ 38 (A); 5 ≤ GAP ≤ 8; 55 ≤ Ton ≤ 85µs; 55 ≤ Tof ≤ 85µs

2.2. Optimization method

The optimizing procedure for the EDD process is illustrated in Fig. 1:

Step 1: Executing EDD experiments using the Box-Behnken method. For the Box-Behnken method, each parameter requires three levels (-1, 0, +1) to present the lowest, middle, and highest ranges. This approach possesses various benefits, such as low experimental costs, saved efforts, and easy implementation. In this work, four factors having three levels and five centre points are employed; hence, 29 experiments are produced.

Step 2: The GPR is used to construct the predictive models of the EDD responses [15].

The GPR is a Bayesian-based probabilistic model to predict the outputs $Y = [y_1, y_2, ..., y_n]$ with the training data $D = \{X, Y\}$ input vector $\mathbf{X} = [\mathbf{x}_1, \mathbf{x}_2, ..., \mathbf{x}_n]$. A GPR model is used to predict the value of a response variable y_{new}, given the new input vector x_{new}, and the training data. The output can be expressed as:

$$y_i(x) = f(x_i) + \varepsilon_i = x^T\beta + \varepsilon_i \quad (4)$$

where $\varepsilon_i = N(0, \sigma^2_n)$. The error variance σ_n^2 and the coefficients β are estimated from the data.

The joint distribution is expressed as:

$$p(f(x)|x_1, x_2, ..x_n) = N(0, K(x, x + \sigma_n^2 I) \quad (5)$$

where $f(x) = [f_1, f_2, \ldots, f_n]$ is vector of latent function values. K(x, x') is the covariance matrix. $\sigma_n^2\mathbf{I}$ introduces the Gaussian noise.

The prior joint distribution of the training output (f) and test output (f^*) are expressed as:

$$p(f, f^*) = N\left[0, \begin{matrix} K_{f,f} & K_{f^*,f} \\ K_{f,f^*} & K_{f^*,f^*} \end{matrix}\right] \quad (6)$$

The independent likelihood can be expressed as:

$$p(y|f) = N(f, \sigma_n^2 I) \quad (7)$$

The posterior distribution with the Gaussian predictive distribution is expressed as:

$$p(f^*|y) = N(\mu_*, \sigma_*^2) \quad (8)$$

where the mean µ and the variance σ^{*2} are given by:

$$\mu_* = K_{f^*,f}(K_{f,f} + \sigma_n^2 I)^{-1} y \quad (9)$$

$$\sigma_*^2 = K_{f^*,f^*} - (K_{f^*,f} + \sigma_n^2 I)^{-1} K_{f,f^*} \quad (10)$$

The squared exponential kernel function between the two input feature vectors is expressed as:

$$K(x_i, x_j) = \sigma_s^2 \exp[-\frac{1}{2}(x_i - x_j)M(x_i - x_j)] + \sigma_s^2 \delta_{ij} \quad (11)$$

where σ_s^2 is the signal variance. M is a diagonal matrix. δ_{ij} is Kronecker's delta function.

The M, σ_s, σ_n are the hyper-parameters of the Gaussian process. These parameters can be learned by maximizing the log likelihood of the training outputs.

$$\theta_{max} = \text{argmax}_{\theta} \begin{Bmatrix} -\frac{1}{2} y^{T} (K + \sigma^2 I)^{-1} y \\ -\frac{1}{2} \log(K + \sigma^2 I) - \frac{n}{2} \log 2\pi \end{Bmatrix} \quad (12)$$

Step 3: The NSGA-II is used to select the optimal data [16]. The NSGA-II is an improved version of the NSGA to minimize computational time and obtain global solutions. The operating principle of the NSGA-II is presented in Fig. 2 and expressed as:

- Randomly generate an initial population P_0.

- The non-domination ranks and crowding distance are used to evaluate the fitness of each individual. The non-dominated set 1 is produced from all the individuals in the objective space. The non-dominated set 2 is formed by individuals exclusively dominated in the set 1, and so on.

- The crowding distance between the individual (d_j) expressed as:

$$d_j = \sum_{m=1}^{M} \frac{f_m^{max\, j+1} - f_m^{min\, j-1}}{f_m^{max} - f_m^{min}} \quad (13)$$

- The crossover operation is used to generate the parent-offspring generation and is expressed as:

$$O_i = 0.5(1+\gamma)P_i + 0.5(1-\gamma)P_{i+1} \quad (14)$$

where O and P are the off spring and parent, γ is a crossover coefficient.

- The mutation operation is used to preserve individual diversity from the obtained generation and is expressed as:

$$O = \begin{cases} O + (2r)^{1/n_m+1} - 1, \text{if } r \le 0.5 \\ O + 1 - (2-2r)^{1/n_m+1}, \text{else'} \end{cases} \quad (15)$$

where r is a random number between 0 and 1, and η_m is the distribution index for mutation.

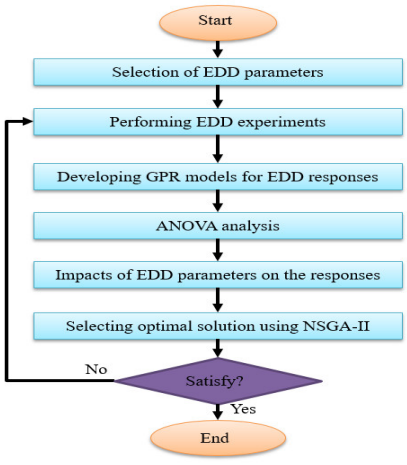

Fig. 1. Optimization approach for the EDD process

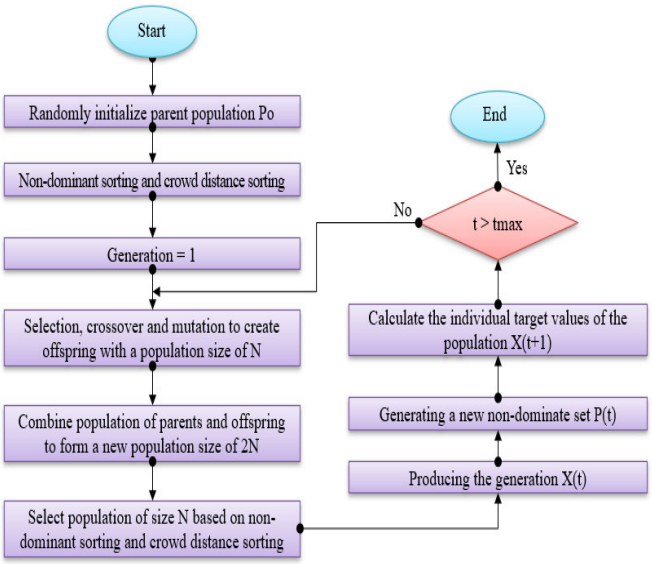

Fig. 2. The operating principle of the NSGA-II

Table 2. Chemical compositions of titanium grade 4

Element	C	N	H	O	Fe	Ti
%	0.07	0.05	0.015	0.40	0.50	Balance

3. EXPERIMENTAL EDD PROCESS

Titanium grade 4 is chosen as an experimental material due to its applications in the airframe and aircraft engine components. The chemical compositions of Titanium grade 4 are shown in Table 2. Each specimen has a length of 200mm, a width of 30mm, and a thickness of 10mm. The specimen's surfaces are ground and polished before the EDD experiments. Two workpiece parts are assembled using a mating interface to measure the drilled length.

The EDD machine entitled CHMER CM-H30A is employed to perform the EDD experiments (Fig. 3). The linear and rotational movements of the electrode are conducted using a servo motor. Dielectric fluid is pumped to the drilling region through the interior channel of the electrode. During the machining process, the debris is removed and the temperature is lowered using high-pressure water. The precise vise vector is used to clamp the workpiece on the machine's table. The copper electrode having a length of 400mm and a diameter of 1mm is used to perform the trials. Once each run reaches the target depth of 15mm, the drilling operation is terminated.

The drilled specimens' dimensions are measured using a Mitutoyo microscope entittled MF176. The average values of the hole diameter and depth are taken from three different points. The representative results for

drilled diameter and length at the No. 10 are presented in Fig. 4.

Fig. 3. EDD Experiments and measurements

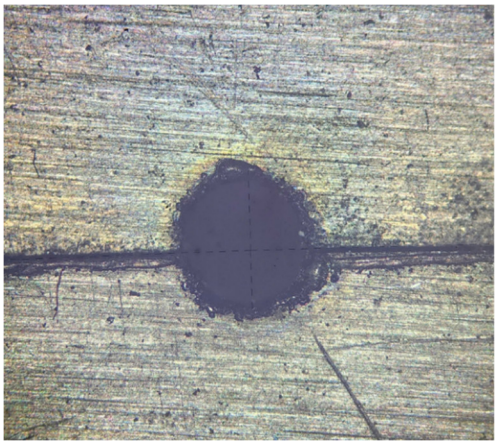

(a) Drilled diameter at the entry

(b) Drilled depth

Fig. 4. The representative results at the No. 10

4. RESULTS AND DISCUSSIONS

4.1. ANOVA results

The DOE matrix and experimental results of the EDD process are given in Table 3.

Table 3. Experimental results of the EDD operation of titanium grade 4

No.	I (A)	G	Ton (µs)	Tof (µs)	HD (mm)	V (mm/min)
1	25	5	85	55	1.283	15.806
2	12	2	70	70	0.665	9.035
3	25	5	70	70	0.532	11.098
4	25	5	70	70	0.535	11.091
5	25	2	70	85	0.585	10.563
6	38	5	70	55	1.363	20.407
7	12	5	55	70	0.339	4.811
8	12	8	70	70	0.268	14.972
9	25	5	55	85	0.286	4.748
10	25	5	70	70	0.534	11.087
11	25	8	70	85	0.338	14.146
12	25	8	85	70	0.833	16.529
13	25	2	70	55	1.215	13.624
14	25	5	85	85	0.668	11.478
15	25	8	55	70	0.289	12.544
16	25	5	70	70	0.537	11.095
17	38	5	70	85	0.717	13.532
18	25	8	70	55	0.633	22.538
19	12	5	70	85	0.286	8.836
20	38	8	70	70	0.744	21.174
21	25	2	85	70	1.131	11.784
22	38	5	85	70	1.366	18.605
23	25	5	40	55	0.753	10.603
24	38	2	70	70	1.136	15.493
25	25	2	55	55	0.704	4.823
26	25	5	70	55	0.536	11.093
27	12	5	85	70	0.664	11.567
28	12	5	70	70	0.612	13.845
29	38	5	55	70	0.806	11.634

The ANOVA results for the HD model are shown in Table 4. The factors having p-value less than 0.05 are significant. As a result, the I, G, Ton, Tof, I^2, Ton^2, and Tof^2 are significant factors (Fig. 5a). The percentage contributions of I, G, Ton, and Tof are 29.26%, 14.62%, 20.61%, and 23.87%, respectively. The contributions of the I^2, Ton^2, and Tof^2 are 2.84%, 3.87%, and 1.63%, respectively.

The ANOVA results for the V model are shown in Table 5. As a result, the I, G, Ton, Tof, I^2, G^2, Ton^2, and Tof^2 are significant factors (Fig. 5b). The percentage contributions of I, G, Ton, and Tof are 22.15%, 20.77%, 20.79%, and 17.44%, respectively. The contributions of the I^2, G^2, Ton^2, and Tof^2 are 4.35%, 6.45%, 3.60%, and 2.45%, respectively.

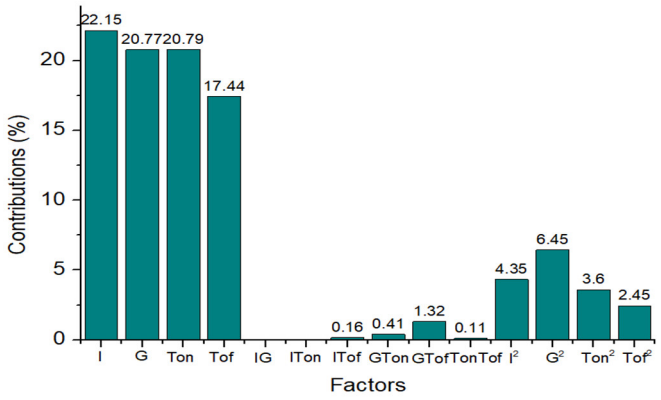

(a) Parametric contributions for the HD model

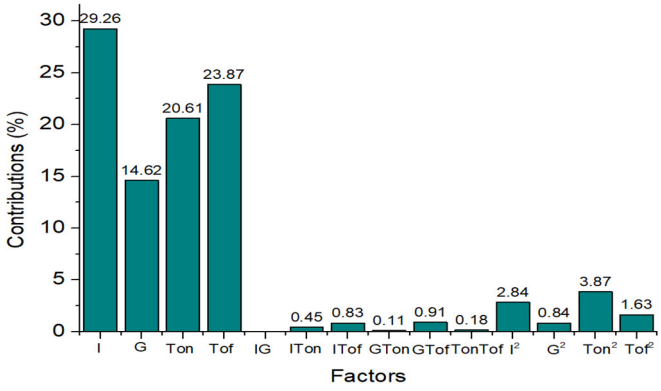

(b) Parametric contributions for the V model

Fig. 5. Parametric contributions for the EDD responses

4.2. Model fitness

The adequacy of the GPR models can be evaluated using the R^2-values. The R^2-values of DH and MRR are 0.9762 and 0.9738, respectively, indicating the significance of the GPR models. Furthermore, as shown in Fig. 6, the observed data is distributed on the straight lines. It is possible to conclude that the measured and predicted values correspond well. As a result, the GPR models' fidelity is satisfactory.

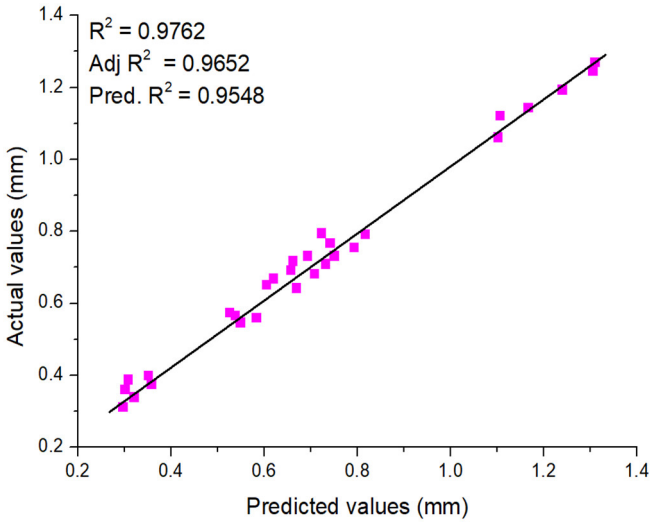

(a) For the HD model

Table 4. ANOVA results for the HD model

Source	Sum of Squares	Mean Square	F value	p-value	Contributions (%)	Remark
Model	2.9512	0.2108	41.0168	< 0.0001		Significant
I	3.9775	3.9775	779.9045	< 0.0001	29.26	Significant
G	1.9870	1.9870	389.6051	< 0.0001	14.62	Significant
Ton	2.8018	2.8018	549.3793	< 0.0001	20.61	Significant
Tof	3.2453	3.2453	636.3281	< 0.0001	23.87	Significant
IG	0.0000	0.0000	0.0054	0.9426	0.00	Insignificant
ITon	0.0606	0.0606	11.8795	0.5286	0.45	Insignificant
ITof	0.1123	0.1123	22.0273	0.2653	0.83	Insignificant
GTon	0.0150	0.0150	2.9446	0.8324	0.11	Insignificant
GTof	0.1231	0.1231	24.1408	0.2248	0.91	Insignificant
TonTof	0.0240	0.0240	4.7118	0.8163	0.18	Insignificant
I^2	0.3864	0.3864	75.7717	< 0.0001	2.84	Significant
G^2	0.1144	0.1144	22.4282	0.2635	0.84	Insignificant
Ton^2	0.5266	0.5266	103.2560	< 0.0001	3.87	Significant
Tof^2	0.2211	0.2211	43.3604	< 0.0001	1.63	Significant
Residual	0.0720	0.0051				
Cor Total	3.0231					
R^2	0.9762					

Table 5. ANOVA results for the V model

Source	Sum of Squares	Mean Square	F value	p-value	Contributions (%)	Remark
Model	533.2681	38.0906	37.1679	< 0.0001		Significant
I	401.5547	401.5547	391.8371	< 0.0001	22.15	Significant
G	376.4913	376.4913	367.3802	< 0.0001	20.77	Significant
Ton	377.0060	377.0060	367.8826	< 0.0001	20.79	Significant
Tof	316.1199	316.1199	308.4698	< 0.0001	17.44	Significant
IG	0.0553	0.0553	0.0540	0.8196	0.00	Insignificant
ITon	0.0390	0.0390	0.0381	0.8481	0.00	Insignificant
ITof	2.9389	2.9389	2.8678	0.364	0.16	Insignificant
GTon	7.4753	7.4753	7.2944	0.1125	0.41	Insignificant
GTof	23.9874	23.9874	23.4069	0.0003	1.32	Significant
TonTof	1.9681	1.9681	1.9205	0.1875	0.11	Insignificant
I^2	78.7884	78.7884	76.8817	< 0.0001	4.35	Significant
G^2	116.9609	116.9609	114.1305	< 0.0001	6.45	Significant
Ton^2	65.2107	65.2107	63.6326	< 0.0001	3.60	Significant
Tof^2	44.3850	44.3850	43.3109	< 0.0001	2.45	Significant
Residual	14.3475	1.0248				
Cor Total	547.6156					
R^2	0.9738					

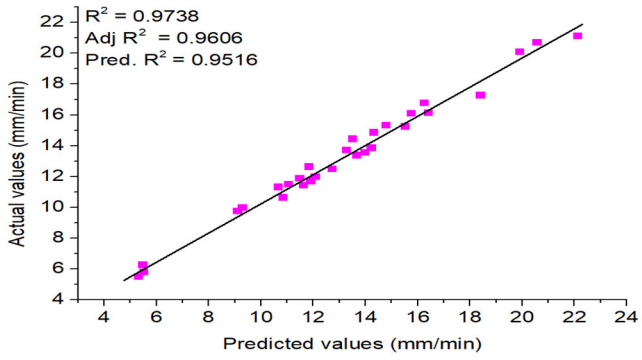

(b) For the V model

Fig. 6. Investigations of the model accuracy for the GPR models

4.3. The effects of process parameters on the technical responses

The effects of EDD parameters on the HD are shown in Fig. 7. As shown in Fig. 7a, a higher I or G increases the hole dilation. The low discharge energy is produced at low values of the I and G resulting in small diameters; hence, a low HD is obtained. In contrast, higher values of the I and G leads to an increase in the discharge energy, more material is melted and evaporated; hence, a higher hole dilation is obtained. As shown in Fig. 7b, a higher Ton increases the hole dilation, while a higher Tof leads to a lower hole dilation. A higher Ton increases discharge energy, leading to more evaporated materials; hence, the HD increases. The longer the Tof, the smaller discharge energy becomes, which decreases the evaporating of materials, leading to a smaller HD.

The effects of EDD parameters on the V are shown in Fig. 8. As shown in Fig. 8a, a higher I or G increases the drilling speed. An increase in the I and G causes higher discharge energy, which leads to an increment in the melting and evaporation; hence, the V increases. As shown in Fig. 8b, a higher Ton increases the drilling speed, while a higher Tof leads to a lower drilling speed. A higher Ton increases the discharge energy, leading to a lower drilling time; hence, the V increases. A higher Tof reduces discharge energy, resulting in higher drilling time; hence, the V decreases.

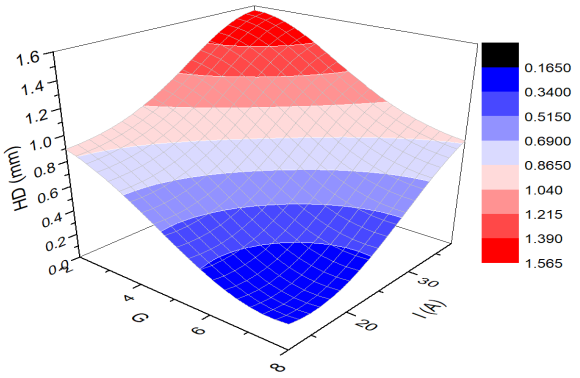

(a) HD versus I and G

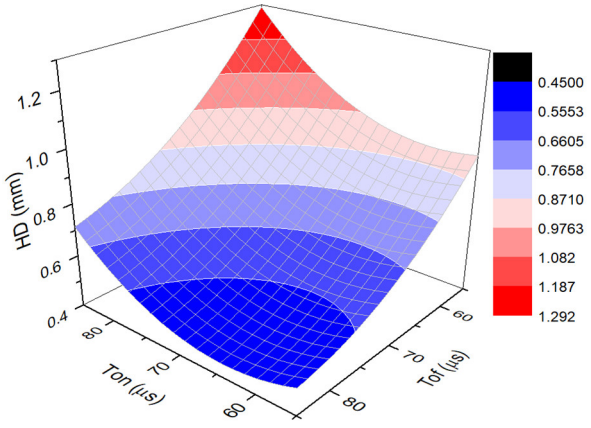

(b) HD versus Ton and Tof

Fig. 7. Interaction effects of each EDD parameters on the HD

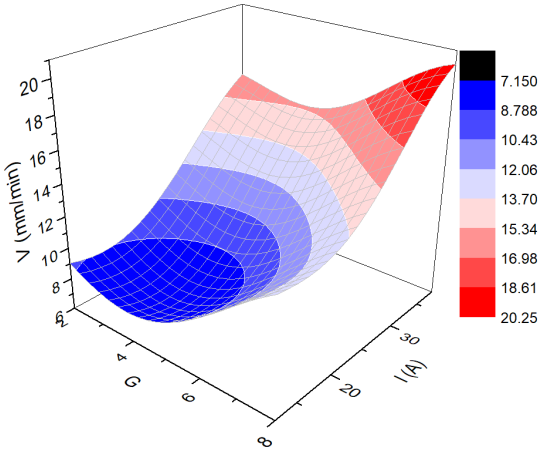

(a) V versus I and G

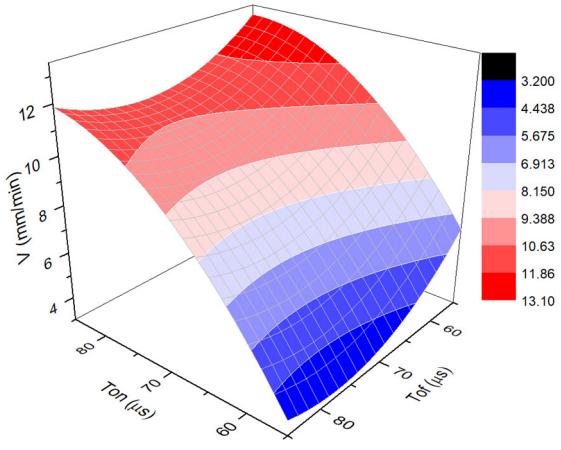

(b) V versus Ton and Tof

Fig. 8. Interaction effects of each EDD parameters on the V

4.4. Optimization results

The NSGA-II is utilized to determine the ideal parameters based on the GPR correlations. The population size, number of generations, crossover probability, crossover distribution index, and mutation distribution index are among the NSGA-II parameters with operational values of 20, 40, 0.9, 10, and 20, respectively.

The Pareto front generated by the NSGA-II algorithm was exhibited in Fig. 9, in which the pink points are feasible solutions. The optimal data are presented in Table 6. The optimal values of the I, G, Ton, and Tof are 13A, 8, 65µs, and 55µs, respectively. The HD is decreased around 32.6% and the V is approximately increased 76.7% at the optimal solution.

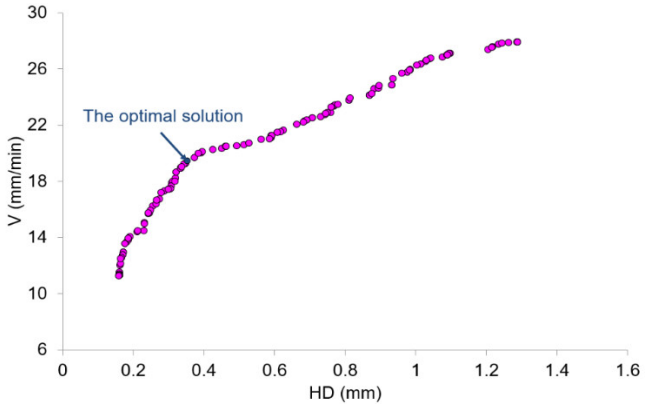

Fig. 9. The Pareto graph generated by NSGA-II

Table 6. Optimization results

Method	Optimization parameters				Responses	
	I (A)	G	Ton	Tof	HD (mm)	V (mm/min)
Initial	25	5	60	60	0.536	11.091
NSGA-II	13	8	65	55	0.361	19.599
Improvement (%)					-32.6	76.7

5. CONCLUSION

In this work, an optimization of the EDD process of titanium grade 4 was conducted to reduce the hole' dilation and improve the drilling speed. The factors considered are the current, gap voltage adjustor, pulse on time, and pulse off time. The GPR was used to propose the predictive models of the EDD responses, while the NSGA-II was used to select the optimal solution. The findings can be expressed as:

1. To reduce the hole dilation, lower values of the current, gap voltage adjustor, and pulse on time should be used, while a higher pulse off time could be applied. To increase the drilling speed, higher values of the current, gap voltage adjustor, and pulse on time should be used, while a lower pulse off time is recommended.

2. For the HD model, the current was found to be the most effective factor, followed by the pulse off time, pulse

on time, and gap voltage adjustor, respectively. For the V model, the current had the highest contribution, followed by the pulse on time, gap voltage adjustor, and pulse off time, respectively.

3. The GPR correlations for the HD and V having R^2-values of 0.9762 and 0.9738, respectively indicate a good correlation between the predicted and experimental values. The models proposed are effectively exhibited the nonlinear relationships in terms of process parameters. The predictive models developed could be used to forecast the response values of the EDD process of titanium grade 4.

4. There is a strong connection between the expected and experimental results, as shown by the GPR correlations for the HD and V, which have R^2 values of 0.9762 and 0.9738, respectively. The developed correlations successfully illustrate the nonlinear interactions between process parameters. The response values of titanium grade 4's EDD process could be predicted using the predictive models created.

5. The optimal values of the I, G, Ton, and Tof were 13A, 8, 65µs, and 55µs, respectively. The HD was decreased around 32.6% and the V was approximately increased 76.7% at the optimal solution.

6. The EDD operators can greatly benefit from the Pareto fronts when choosing the right parameters to reduce the hole dilatation and improve the drilling rate. Choosing the right parameters can reduce the amount of efforts, the cost of drilling, and the time needed to complete the process.

7. The impacts of the tool rotational speed, fluid pressure, and linear speed on the hole dilation and drilling speed will be explored in next works.

REFERENCES

[1]. Kumar A., Pradhan M.K., "An ANFIS modelling and genetic algorithm-based optimization of through-hole electrical discharge drilling of Inconel-825 alloy," *J. Mater. Res.,* 38: 312327, 2023.

[2]. Harane P.P., Unune D.K., et al., "Multi-objective optimization for electric discharge drilling of waspaloy: A comparative analysis of NSGA-II, MOGA, MOGWO, and MOPSO," *Alex. Eng. J.*, 99: 1-16, 2024.

[3]. Nguyen T.T., Tran V.T., Le M.T., "Comprehensive optimization of the electrical discharge drilling in terms of energy efficiency and hole characteristics," *Int. J. Precis. Eng. Manuf.*. 23: 807–824, 2022.

[4]. Chen S.H., Huang K.T., "Deep hole electrical discharge machining of nickel-based Inconel-718 alloy using response surface methodology," *Int. J. Adv. Manuf. Technol.,* 117: 3281–3295, 2021.

[5]. Pandey G.K., Yadav S.K.S., "Experimental investigation to evaluate the effect of low frequency vibration on performance of vibration assisted electrical discharge drilling of titanium alloy," *Int. J. Interact. Des. Manuf.*, 2023.

[6]. Ahuja N., Batra U., Kumar K., "Multicharacteristics optimization of electrical discharge micro hole drilling in Mg alloy using hybrid approach of GRA-regression-PSO," *Grey. Syst.*, 11: 136-151, 2021.

[7]. Jeevamalare J., Sundaresan R., Jayaraj J., "On the influence of electrical discharge drilling parameters and per-formance measures of Inconel 718 Superalloy - a Study," *Mechanika*, 27:483-491, 2021.

[8]. Machno M., "Investigation of the machinability of the inconel 718 superalloy during the electrical discharge drilling process," *Materials,* 13: 3392, 2020.

[9]. Nguyen T.T., Tran V.T., Mia M., "Multi-response optimization of electrical discharge drilling process of SS304 for energy efficiency, product quality, and productivity," *Materials*, 13: 2897, 2020.

[10]. Dilip D.G., Panda S., Mathew J., "Characterization and parametric optimization of micro-hole surfaces in micro-EDM Drilling on Inconel 718 superalloy using genetic algorithm," *Arab. J. Sci. Eng.,* 45: 5057–5074, 2020.

[11]. Yadav U.S., Yadava V., "Experimental investigation on electrical discharge diamond drilling of nickel-based superalloy aerospace material," *Proc. Inst. Mech. Eng.,* 231: 1160-1168, 2015.

[12]. Singh N.K., Poras A., "Electrical discharge drilling of D3 die steel using air assisted rotary tubular electrode," *Mater today-Proc.,* 5: 4392-4401, 2018.

[13]. Yadav V.K., Kumar P., Dvivedi A., "Performance enhancement of rotary tool near-dry EDM of HSS by supplying oxygen gas in the dielectric medium," *Mater. Manuf. Process,* 16: 1832-1846, 2019.

[14]. Pattanayak S., Sahoo A.K., Sahoo S.K., "CFRP composite drilling through electrical discharge machining using aluminum as fixture plate," *Proc. Inst. Mech. Eng., Part C,* 236:5468-5483, 2022.

[15]. Hu K., Huang Q., Wang L., et al., "Optimization of multi-track, multi-layer laser cladding process parameters using Gaussian process regression and improved multi-objective particle swarm optimization," Int. J. Adv. Manuf. Technol., 137: 3503-3523, 2025.

[16]. Kushwaha K., Jana R.K., Dutta P., "*Multi-objective multi-item solid transportation problem using penalty-based NSGA-II: a case study on fertilizer transportation in India,"* Sādhanā 50: 67, 2025.

THÔNG TIN TÁC GIẢ

Vũ Ngọc Nhạ[1], Lê Văn An[2], Lương Thị Lan Hương[3], Nguyễn Trung Thành[1]

[1]Khoa Cơ khí, Đại học Kỹ thuật Lê Quý Đôn

[2]Khoa Kỹ thuật và Công nghệ, Đại học Nguyễn Tất Thành

[3]Khoa Ngoại Ngữ, Đại học Kỹ thuật Lê Quý Đôn